Cholesterol and phosphatidylserine are engaged in adenoviral dodecahedron endocytosis

Marta Jedynak[1], Remigiusz Worch[2]*, Małgorzata Podsiadła-Białoskórska[1], Jadwiga Chroboczek[1,3], Ewa Szołajska[1]*

1 Institute of Biochemistry and Biophysics, Polish Academy of Sciences, ul. Pawińskiego 5a, PL 02-106 Warsaw, Poland

2 Institute of Physics, Polish Academy of Sciences, Al. Lotników 32/46, PL 02-293 Warsaw, Poland

3 TheREx TIMC-IMAG UJF-CNRS UMR 5525, 38706 La Tronche Cedex, France

* corresponding authors: EwaSzolajska, ewasz@ibb.waw.edu.pl, tel. +48 22 592 24 20;

RemigiuszWorch, remiwo@ifpan.edu.pl, tel. +48 22 843 66 01, ext. 2204

Abstract

Adenoviral dodecahedron is a virus-like particle composed of twelve penton base proteins, derived from the capsid of human adenovirus type 3. Due to the high cell penetration capacity, it was used as a vector for protein, peptide and drug delivery. Two receptors are known to be involved in the endocytic dodecahedron uptake, namely αv integrins and heparan sulfate proteoglycans. Since it has been observed, that dodecahedron efficiently penetrates a wide range of cancer cells, it suggests that other cellular compounds may play a role in the particle endocytosis. To shed some light onto the interactions with membrane lipids and their potential role in dodecahedron entry, we performed a series of experiments including biochemical assays, fluorescence confocal imaging of giant unilamellar vesicles and surface plasmon resonance, which indicated specific preference of the particle to anionic phosphatidylserine. Experiments performed on cholesterol-depleted epithelial cells showed that cholesterol is essential in the endocytic uptake, however a direct interaction was not observed. We believe that the results will allow to better understand the role of lipids in dodecahedron entry and to design more specific dodecahedron-based vectors for drug delivery to cancer cells.

Abbreviations: BSA - bovine serum albumin; CL - cardiolipin; Dd - dodecahedron; ECL - enhanced chemiluminescence; FBS - fetal bovine serum; GUV - giant unilamellar vesicle; HAd3 - human adenovirus serotype 3; HRP - horseradish peroxidise; HSPG - heparan sulphate proteoglycan; LUV- large unilamellar vesicles; mβCD - methyl-β-cyclodextrin; NHS -N-hydroxysulfoxuccinimide; PA- phosphatic acid; Pb - penton base protein; PBS - phosphate buffered saline; PC - phosphatidylcholine; PE- phosphatidylethanolamine; PG - phosphatidylglycerol; PI- phosphatidylinositol (PtdIns4); PIP_2- PtdIns(4,5)P; PIP_3- PtdIns(3,4,5)P; PIP_4- PtdIns(4)P; PS- phosphatidylserine; RU- response units; SA- 3-sulfogalactosylceramide (sulfatide); SDS-PAGE - sodium dodecyl sulfate polyacrylamide gel electrophoresis; SPR - surface plasmon resonance; TMB - 3,3',5,5'-tetramethylbenzidine;VLP - virus-like particle

Graphical abstract

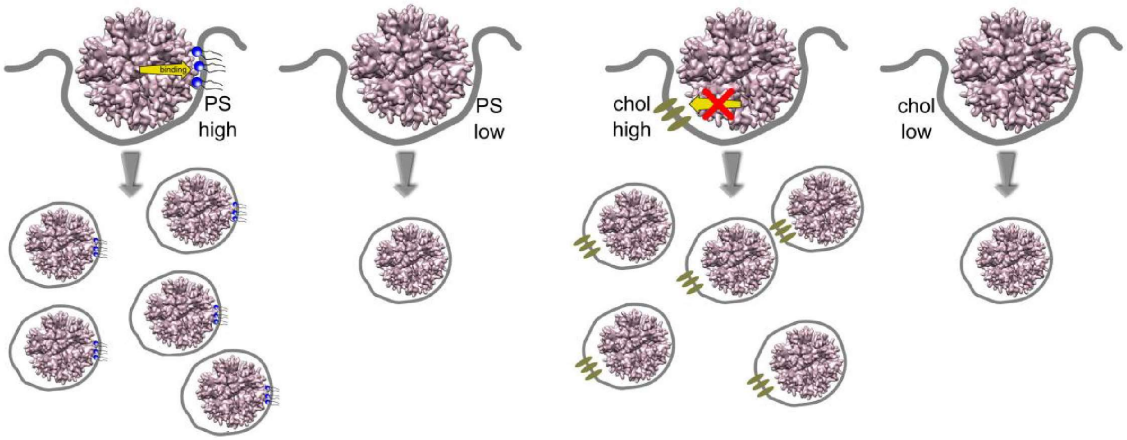

Highlights

- Adenoviral dodecahedron (Dd) is an efficient delivery vector
- Cell type specificity of Dd is not well understood
- Dd displays specific affinity to phosphatidylserine
- Cholesterol is indirectly involved in Dd endocytosis

Keywords

virus-like particles; protein-lipid interactions; giant unilamellar vesicles; artificial model membranes; fluorescence confocal microscopy; phosphatidylserine

1. Introduction

One of the approaches in targeted drug delivery is the application of nanocarriers that deliver chemotherapeutic agents directly to cancer cells. Virus-like particles (VLP) are being developed as drug delivery vectors because they are biodegradable, carry no genetic information and efficiently penetrate plasma membrane. In particular, adenoviral dodecahedron (Dd) has been used as a vector for intracellular delivery of various cargos such as: peptides [1], proteins [2] and anticancer agents [3,4]. Dd is composed of twelve copies of the viral capsid protein, pentameric penton base (Pb), which is responsible for virus cell entry [5]. During cell entry Dd utilizes receptor-mediated endocytosis through the interaction between its RGD amino acids sequences and αv integrins as well as between

KQKR basic amino acids sequences and negatively charged heparan sulfate proteoglycans (HSPGs) present on the surface of majority mammalian cells [6,7]. The KQKR motif is concomitantly involved in intergrin binding [8]. Similarly to HAd3, Dd escapes from the endosome into cytoplasm where it accumulates in the vicinity of the nuclear membrane [5]. Dd quite easily penetrates epithelial and endothelial cells, astrocytes or dendritic cells, leukocytes and cancer cells including drug resistant cell line [1,2,5,9,10]. However, some differences regarding Dd ability to penetrate particular cell types have been noticed. Although, lipids are the main components of cellular membranes, the interactions of adenoviral penton base protein with lipids has not been described hitherto. To fill this gap, we examined interactions between Dd and lipid species naturally occurring in cell membranes. The experiments performed on cholesterol-reduced epithelial cells demonstrated the crucial role of cholesterol in efficient Dd endocytosis. We conducted various analyses of direct interactions between Dd and lipids with a special interest in using artificial membrane systems such as large (LUVs) and giant unilamellar vesicles (GUVs). Thanks to the lack of compositional complexity and cellular mechanism, we take advantage of their membrane controllable composition, size and geometry. Biochemical assays in conjunction with fluorescence confocal imaging of Dd interaction with GUVs ruled out a direct interaction with cholesterol, however indicated specific preference of Dd to anionic phospholipid - phosphatidylserine (PS). The affinity of Dd to PS may potentially have implications for Dd-based drug delivery system application in cancer treatment, since is known that PS, which, under homeostasis in healthy cells is localized in the internal surface of the cell membrane, is aberrantly exposed on the outer membrane leaflet of tumor cells and blood vessels [11]. Our preliminary data suggest that PS may be involved in Dd endocytosis in viable cancer cells exposing this anionic lipid on the surface, as the Annexin V specific binding to PS, prior the incubation with Dd, significantly decreased Dd entry capacity.

2. Material and Methods

2.1. Materials

Amplex Red cholesterol assay kit and Alexa Fluor 647 protein labeling kit were purchased from Invitrogen Molecular Probes. Polyclonal rabbit anti-Dd serum was obtained in the laboratory [5]. Alexa Fluor 555 conjugated chicken anti-rabbit IgG was purchased from Molecular Probes, and anti-rabbit HRP - from Sigma. TMB detection kit and ECL Western Blotting Substrate were purchased from Pierce. PC (1-Palmitoyl-2-oleoyl-sn-glycero-3-phosphocholine), PS (1-palmitoyl-2-oleoyl-sn-glycero-3-phosphatidylserine), cardiolipin (CL) cholesterol, phosphatidylglycerol (PG), phosphatidylinositol (PI), phosphatidylinositol-3,4,5-triphosphate (PIP_3) were purchased from Avanti Polar Lipids Ltd (Alabaster, AL) or its distributors and used with no further purification. Fatty acids-free BSA and other chemicals were purchased from Sigma. Annexin V and annexin binding buffer

(10mM Hepes, 2.5mM CaCl2, 140mM NaCl) were purchased from Clontech (TaRaKa). ProLong Glass Antifade Mountant was purchased from Invitrogen.

2.2. Cells

HeLa cells were purchased from ATCC and were cultivated in DMEM supplemented with GlutaMAX, 10% FBS and streptomycin/penicillin (100 µg/ml and 100 IU/ml, respectively). Human astrocytoma cells U-251 MG (formally known as U-373 MG) were purchased from Sigma and were cultivated in DMEM supplemented with 1% Non Essential Amino Acids (NEAA), 10% FBS and streptomycin/penicillin (100 µg/ml and 100 IU/ml, respectively).

2.3. Protein expression and purification

Dd was produced in the baculovirus expression system following the manufacturer's protocol (FlashBacGold, Oxford Expression Technologies). After 48 h expression in *Trichoplusiani* cells (2 x 10^6 cells/ml infected with recombinant baculovirus at multiplicity of infection 4), Dd was purified from the cell lysate's supernatant by size exclusion chromatography followed by anion exchange chromatography, as described in previous work [12]. Dd preparations were concentrated using Amicon Ultra concentrators (Merck Millipore), protein concentration was determined by NanoDrop ND-200 UV-Vis Spectrophotometer (Thermo Scientific) and SDS-PAGE analysis in the presence of known amounts of BSA. The homogeneity of preparations were analyzed by SDS-PAGE. The assembly status of purified VLPs was analyzed by electron microscopy and native agarose electrophoresis.

2.4. Dd labeling

The Alexa Fluor 647 reactive dye has a succinimidyl ester moiety that reacts efficiently with primary amines of protein lysine residues to form stable dye-protein conjugates. Dd labeling was performed according to the manufacturer's protocol. Briefly, 50 µl of 1 M bicarbonate was added to 1 ml of Dd (1 mg/ml) in PBS to adjust the pH of the reaction. Subsequently the protein solution was combined with the reactive dye Alexa Fluor 647 (Dd-Alexa 647). The mixture was stirred for 3-5 h at room temperature. The resulting conjugates were purified by the extensive dialysis against PBS. The absorbance of the conjugate solution was measured at 280 nm and 650 nm (Synergy HTi plate reader, BioTek, Winooski VT, USA). Degree of labeling was calculated according to manufacturer's protocol.

2.5. Cholesterol depletion

HeLa cells were grown in 6-well plates for 24 h at 37 °C to 80% confluence. The cellular cholesterol was reduced with 25 mM mβCD diluted in RPMI containing 0.2 % BSA, for 20 min at RT. Cells were

detached using 0.02% DTA in PBS (Versene, Lonza) at 4 °C for 40 min and then centrifuged at 1,000 x g for 2 min. Cell pellets were resuspended in 100 µl of Amplex Red solution and homogenized using a 20-gauge needle. Cholesterol was measured enzymatically by determination of cholesterol oxidase activity using an Amplex Red readout at 560 nm excitation and 590 nm emission using Synergy HTi plate reader (Biotek, Winooski VT, USA) according to the manufacturer's instructions. The level of cholesterol in treated and control cells was calculated according to manufacturer's protocol. The result is an average from triplicates.

2.6. Dd penetration of mβCD-treated cells

HeLa cells were grown overnight to 80% confluence on the poly-D-lysine-coated coverslips (BD BioCoat) placed in the individual wells of the 24-well plate (Greiner Bio-one). Cholesterol depletion was carried out as described above. After three washes with PBS, serum-free DMEM with the addition of Dd at the final concentration 20 μg /ml, was applied to cells non-treated (control endocytosis) and treated with 25 mM methyl-β-cyclodextrin (mβCD) and incubated for 2 h at 37 °C. Additional control cells were incubated with Dd (20 μg/ml) for 2 h at 4 °C (control endocytosis inhibition). Then, cells were rinsed three times with PBS and fixed with 100% cold methanol for 20 min at -20°C. Subsequently, cells were blocked with 5% BSA in PBS for 1 h at 37 °C, next incubated for 1 h at RT with the polyclonal rabbit anti-Dd serum diluted 1:1,000 and washed three times with PBS. After that cells were incubated with the Alexa Fluor 488- conjugated chicken anti-rabbit IgG diluted 1:500 for 1 h at RT, washed with PBS and finally stained with DAPI (5 µg/ml) for10 min at RT. Coverslips were sealed in a closure medium (Mowiol, Fluka) and left for 24 h at 4 °C. Images were collected with EZ-C1 Nikon CLSM attached to inverted microscope Eclipse TE2000 E using oil immersion objective ×60, Plan Apo 1.4NA (Nikon). DAPI and Alexa Fluor fluorescence were excited at 408 and 488 nm, and emission was measured at 430-465 and 500-530 nm, respectively. All images were collected at 512×512 resolution and zoom 2.0. The images shown in Fig. 1A were selected as representative from three independent experiments and were processed with EZ-C1 Viewer and adjusted simultaneously. Statistical analysis was performed with Python *scipy* statistical libraries.

2.7 Dd internalization after PS binding with Annexin V

U-251 cells were grown overnight to 80% confluence on 4-well chamber slides (BD Falcon). After three washes with annexin binding buffer, 5 µl of Annexin V-FITC (AnnV) (20 µg/ml in Tris-NaCl) diluted in 200 µl of annexin binding buffer was added to indicated wells and incubated in dark for 15 min. Subsequently, AnnV was removed and cells were washed with annexin binding buffer. Aliquots of 10 µg Dd diluted in annexin binding buffer at the final concentration of 20 µg/ml, were applied to cells non-treated (control of endocytosis) and treated with AnnV respectively and incubated for 2 h at 37 °C. Simultaneously, control cells with or without AnnV preincubation respectively were incubated

with Dd (20 µg /ml) for 2 h at 4 °C (control endocytosis inhibition). Then, cells were rinsed three times with annexin binding buffer and fixed with 2 % formaldehyde. Subsequently, cells were blocked with 5% BSA in PBS for 1 h at 37 °C, next incubated for 1 h at RT with the polyclonal rabbit anti-Dd serum diluted 1:1,000 and washed three times with PBS. After that cells were incubated with the Alexa Fluor 488- conjugated chicken anti-rabbit IgG diluted 1:500 for 1 h at RT, washed with PBS and finally stained with DAPI (5 µg/ml) for10 min at RT. Slides were sealed with an antifade mountant and left for 24 h at 4 °C. Images were collected with EZ-C1 Nikon CLSM attached to inverted microscope Eclipse TE2000 E using oil immersion objective ×60, Plan Apo 1.4NA (Nikon). DAPI and Alexa Fluor fluorescence were excited at 408 and 488 nm, and emission was measured at 430-465 and 500-530 nm, respectively. All images were collected at 512×512 resolution and zoom 2.0. The images that are shown in Fig. 6 were selected as representative and were processed with EZ-C1 Viewer and adjusted simultaneously. Statistical analysis was performed with Python *scipy* statistical libraries.

2.8. Corrected total cell fluorescence measurement

The fluorescence intensity was determined by counting pixels using ImageJ and the corrected total cell fluorescence (CTCF) average was calculated using Excel and the formula: CTCF= the value of integrated density - (area of selected cell x mean fluorescence of background readings).

2.9. Protein Lipid overlay assay

Lipid Strips (Echelon Biosciences) spotted with 100 pmol of fifteen different biologically important membrane lipids were used and the assay was performed according to the manufacturer's protocol. Briefly, the membrane was blocked with PBS containing 0.1% Tween-20 and 3% BSA (blocking buffer) for 1h at RT. Subsequently, the blocking buffer was exchanged with 5 ml of the blocking buffer containing either Dd (30 µg/ml) or Dd-Alexa647 conjugate (30 µg/ml). The incubation was carried out for 1 h at RT with gentle agitation. Negative control samples were incubated with the blocking buffer alone or with protein (30 µg/ml) without primary antibody. After three washes with PBS containing 0.1% Tween-20 (PBS-T), the primary polyclonal rabbit anti-Dd serum diluted 1:40,000 in the blocking solution was added and incubated for 1 h at RT with gentle agitation. After washing with PBS-T, the anti-rabbit HRP diluted 1:100,000 in blocking solution was added and incubated for 1 h at RT with gentle agitation. The bound protein was detected with ECL. Three independent experiments were performed for Dd as well as Dd-Alexa647. Quantitative analysis of dot blot was performed with ImageJ.

2.10. Colorimetric assay on ELISA Strip

For absorbance measurements Optically Clear Lipid Snoopers (Avanti Polar Lipids) were used. Each 8-well strip contained 1 nmol of pure lipid. First, 200 µl of blocking solution (PBS containing 3% of fatty acids free BSA) was added to each well and incubated for 1 h at RT with gentle shaking. After three washes with 200 µl PBS pH 7.4 (washing solution) the ELISA Strips were incubated with Dd. Indicated amounts of Dd (1, 2, 3 and 5 pmol respectively) diluted in 50 µl of blocking buffer were applied on strips and incubated for 2 h at RT with gentle shaking. After three washes with 200 µl of washing solution, the primary antibody (polyclonal rabbit anti-Dd serum) diluted 1:40,000 in blocking solution (50 µl per well) was added and the incubation was carried out for 1 h at RT. Subsequently strips were washed three times with washing solution and HRP-conjugated secondary antibody diluted 1:100,000 in blocking solution was added and incubated for 1 h at RT with gentle agitation. Following three washes and removal of the final wash solution, bound Dd was detected with TMB detection kit (100 µl/well). After 15 min, the enzymatic reaction was stopped with 2 M H_2SO_4, followed by the colour change from blue to yellow. The absorbance was measured at a wavelength of 450 nm in Synergy HTi plate reader (Biotek). Signals for blank controls were subtracted. The apparent binding constants K_d^{app} were obtained from non-linearhyperbolic curve fits to the averaged (triplicates) A_{450} values:

$$A450([Dd]) = (A_{inf} \bullet [Dd])/(K_d^{app} + [Dd])$$

A_{inf} denotes the asymptote of the hyperbola.

2.11. GUV preparation and imaging

GUVs were prepared by electroformation [13] using Pt wire electrodes in homemade Teflon chambers. Individual lipid species were prepared as 40 mol% mixtures with POPC, with the exception of PIP3 for which the amount was reduced to 20 mol% due to inefficient electroformation for the higher molar ratio. We applied 5 μl of 1 mg/ml lipid mixture in chloroform on each wire that was cleaned beforehand in ethanol in an ultrasonic bath, followed by 15 min of drying at 37 °C for solvent evaporation. The chamber was filled with 350 μl of 0.3 M sucrose and an alternating current of 3 V (peak-to-peak) was applied in two steps: 10 Hz for 2 h and 2 Hz for 0.5 h. 40 μl of GUVs solution was transferred to a chambered 8-well cover glass #1 (Lab Tek, Nunc). Each chamber was filled with 125 μl of 20 mM Hepes, pH 7.4 containing 0.1 mM EDTA, 150 mM NaCl. Under such conditions GUVs, which are filled with sucrose, sediment at the bottom of the chamber with no further need of immobilization. To each well 2-5 μl of Dd stock (0.175 mg/ml) in the same buffer was added and incubated for 1 h at RT. Primary polyclonal rabbit anti-Dd serum diluted 1:1,200 in the same buffer was added and incubated for 1 h at RT, followed by incubation with the secondary antibody (diluted 1:300) labelled with Alexa Fluor 555. Imaging of GUVs was performed using the Zeiss LSM780 microscope with a C-Apochromat 40x, 1.2 NA water immersion objectives, MBS 488/561/633 dichroic mirrors, and two laser lines: 488 nm (Ar/Ion), 561 nm (DSSP) for excitation of green and

orange fluorophores, respectively. Emission was registered in GaAsP or PMT detectors with proper spectral ranges. 512x512 pixel images were analyzed in ImageJ (http://imagej.nih.gov/ij/). Typically 20-30 were imaged for given GUV lipid composition with representative images presented in figures.

2.12. LUV preparation

Desired amounts of lipids in chloroform or chloroform/methanol 2/1 (v/v) were dried under a stream of nitrogen and overnight under vacuum, followed by rehydration with appropriate buffer to 2-10 mg/ml concentration. The dispersion was frozen and thawed in liquid nitrogen and 40 °C water bath at least 6 times, followed by extrusion (21 times) through polycarbonate filters with 100 nm pores (Whatman) using Avanti Mini Extruder.

2.13. SPR measurements

The Sensor Chip L1 surface was primed in Biacore 3000 with PBS and washed by two short injections of 2:3 (v/v) isopropanol:50 mM NaOH. LUVs (PC or PC/PS 60/40 mol% in PBS) at concentration of 0.5 mM with respect to phospholipids were adsorbed at a flow rate of 5 µl/min for 10 min. Typically, 4.000-5.800 RU (response units) were adsorbed. Injections with Dd were made after the response stabilization. Increasing amounts of Dd (1.8-14.4 μg/ml of Dd in PBS) were injected. PBS was used in all trials as running buffer. Sensogram analysis was performed by home-developed scripts in Python (www.python.org).

3. Results

3.1. Cholesterol depletion impairs Dd endocytosis

To validate whether membrane components other than known Dd receptors may be engaged in Dd endocytosis, we initially focused our attention on cholesterol as a potential factor mediating Dd cell entry. For cholesterol depletion in HeLa cells we used methyl-β-cyclodextrin (mβCD). The analysis of Dd endocytosis in mβCD-treated and control HeLa cells was performed using confocal microscopy imaging. Treatment of HeLa cells with 25 mM mβCD resulted in reducing cholesterol level by half in comparison to control cells, as indicated by Amplex Red quantification (Fig. 1C). Unlike the control cells, incubated with 10 µg Dd at 37°C (Fig. 1A, upper panel), Dd endocytosis in cholesterol-depleted cells was inhibited, although not completely, since a half of the remaining cholesterol was sufficient to induce Dd internalization to some extent (Fig. 1A, lower panel). Statistical analysis based on three independent experiments (Fig. 1B) demonstrated that cholesterol depletion with 25 mM mβCD, resulted in about 60% inhibition of Dd endocytosis.

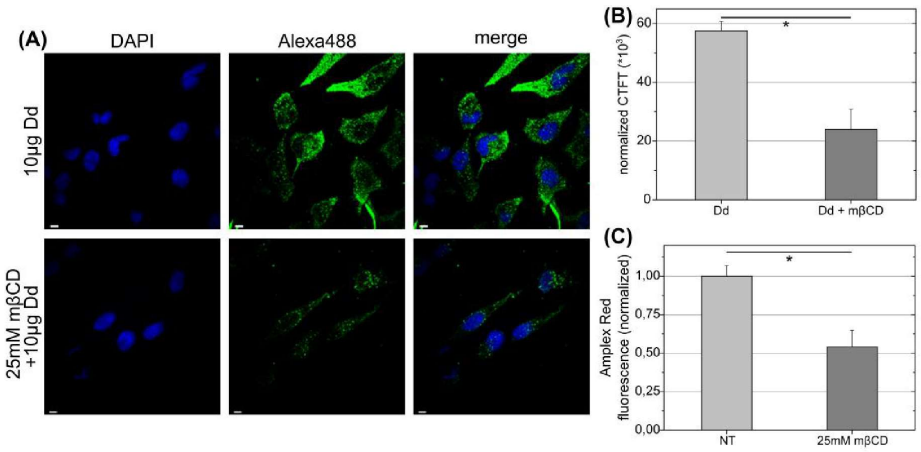

Fig. 1. Confocal microscopy imfing of Dd endocytosis to cholesterol-depleted cells. (A) Representative confocal microscopy images of HeLa cells incubated with 10 µg of Dd at 37°C for 2 h (upper panel) and cells treated with 25 mM mβCD prior to incubation with Dd at 37 °C (lower panel). Intracellular Dd was recognized with anti-Dd and secondary Alexa Fluor 488-conjugated (Alexa488) antibodies (green). Cell nuclei were stained with DAPI (blue). All images were adjusted simultaneously using EZ-C1 Viewer (Nikon). Scale bar 10 µm. (B) Corrected total cell fluorescence (CTCF) measurement for HeLa cells related to incubation with 10 µg of Dd at 37 °C for 2 h (Dd) and with preincubation with 25 mM mβCD (mβCD + Dd). Data represent mean ± s.d. for three independent experiments. (C) Reduction of cellular cholesterol with 25 mM mβCD. The level of cholesterol was measured enzymatically (see Materials and Methods) and expressed as a percentage of cellular cholesterol in mβCD-treated cells relative to non-treated cells. Data represents average and standard deviation from three independent measurements (* - *p*-value < 0.001, two-sided T-test).

3.2. Screening of Dd-lipid interactions

To verify direct interactions between Dd and cholesterol as well as other common lipids found in cell membranes, we performed protein-lipid overlay assay with lipid strips, used widely as a first-assessment experiments on protein-lipid binding [14]. Here, fifteen different lipids are immobilized on a solid support (Fig. 2 A) and protein is detected with antibodies and chemiluminescence. Dd at the concentration of 30 µg/ml was detected on spots with phosphatidylserine (PS) and cardiolipin (CL) and to a much lesser extent with other anionic phospholipids such as phosphatidylinositol (PI), phosphatidylinositol-4-phosphate (PIP), phosphatidylinositol-4,5-diphosphate (PIP_2) and phosphatidylinositol-3,4,5-triphosphate (PIP_3) (Fig. 2C, 2E). Nevertheless, direct interaction with cholesterol was not observed in any of the experiments (Fig 2C and 2E). The negative control showed no false positive signals (Fig. 2B).

We also intended to evaluate the influence of Dd surface side chain modification on lipid binding. For that purpose we incubated membrane strips with Dd conjugated via primary amine of lysine side chains with N-hydroxysuccinimidyl ester (NHS) of Alexa Fluor647 dye (Dd-Alexa647 conjugate). For Dd-Alexa647 conjugate used at concentration 30 µg/ml we observed significantly decreased signals for PS as well as with other lipids as compared to unmodified Dd. The increase of signal with PIP is unspecific (Fig. 2F), since a dark spot was observed only in one of the three repetitions. We observed quite large variations between individual experiments and decided to use alternative methods to fully characterize Dd lipid binding partners of and to rule out the unspecific ones.

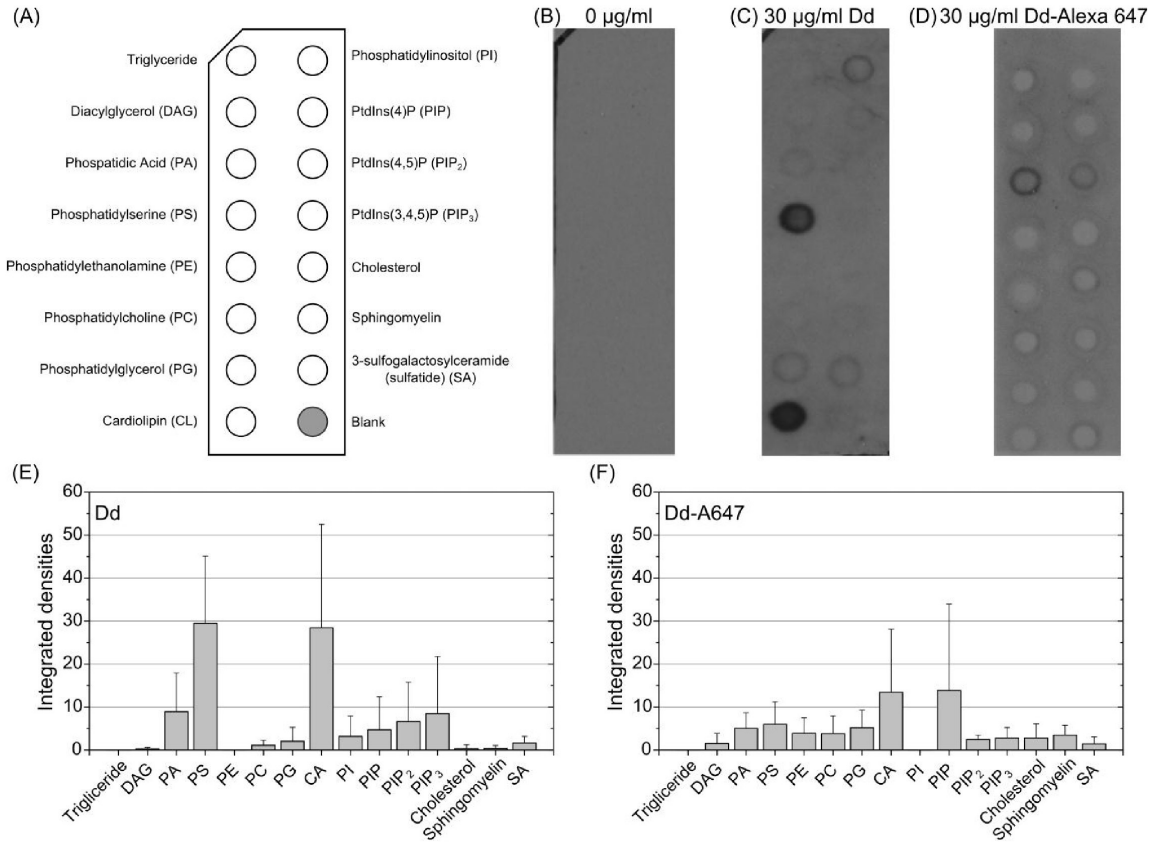

Fig. 2. Protein-lipid overlay assay. (A) Schematic diagram of the membrane strip with immobilized phospholipids in 100-pmole per spots (Membrane Lipid Strips, Echelon). Strips were incubated with blocking buffer without protein (negative control) (B), with 30 μg/ml Dd (C), and with 30 μg/ml Dd-Alexa647 conjugate (D). Lipid-bound Dd and Dd-Alexa647 were detected with polyclonal rabbit anti-Dd antibody followed by a goat-anti-rabbit-HRP antibody. Quantitative analysis of dot blots with 30 μg/ml Dd (E), and with 30 μg/ml Dd-Alexa647 conjugate (F). Data represents mean values ± standard

deviation from three independent experiments.

Intrigued by the above findings showing the preference of Dd mostly to PS and CL, and to a lesser extent to other anionic lipids, we decided to continue the experiments and performed colorimetric assays on ELISA strips allowing for easier data collection and for the possibility of concentration dependency registration. The obtained (blank-subtracted) absorbance values plotted versus the amount of Dd were applied for constructions of binding curves (Fig. 3A, B). We analyzed PS, phosphatidylglycerol (PG), sulfatide (SA), phosphatidylinositol lipids with net charge from -2 (PIP) to -5 (PIP_3) under physiological pH conditions [15], and neutral zwitter-ionic phosphatidylcholine as a negative control. Unfortunately, cardiolipin was not available on ELISA strips. In the case of PC, PG, PS and SA we were able to perform non-linear curve fitting of a simple hyperbolic binding isotherm and to extract apparent binding constants (K_d^{app}). Being aware that volume is poorly controlled in such type of experiments and propagates into large errors of K_d^{app}, we treat the absolute numbers with caution and rather on a semi-quantitative level. Nevertheless, the curvatures for PS, PG and SA (Fig. 3A) corresponded to lower K_d^{app} (higher affinity), as compared to the one for PC (Fig. 3C). The lipids, regarding their K_d^{app} (as a ratio with K_d^{app} for electrically neutral PC), could be ordered as following: PS (~10-fold lower K_d^{app}), SA (~5-fold lower) and PG (~3-fold lower). The data for phosphatidylinositols did not permit a conclusive K_d^{app} determination, since the binding curves in Fig. 3B are linear and indicate rather nonspecific binding of the particles to PIPs, consistently to the result obtained for protein-lipid overlay (Fig. 2C and 2E).

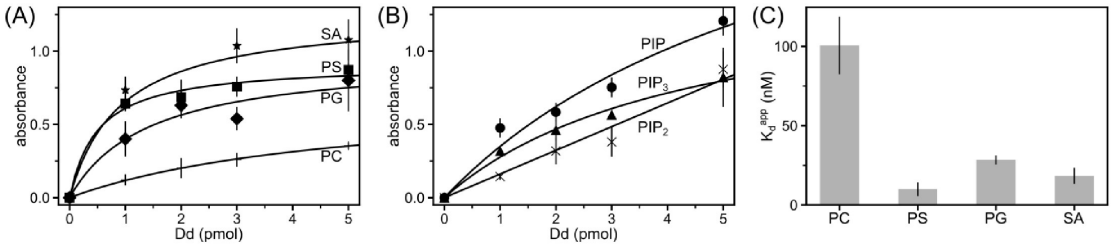

Fig. 3. Colorimetric assay. ELISA Strips immobilized (A) PC, PS, PG, SA, (B) PIP, PIP_2, PIP_3 (1 nmol each) were probed with 1, 2, 3 and 5 pmoles of Dd respectively. Dd was recognized with rabbit anti-Dd antibody followed by a goat-anti-rabbit -HRP antibody. Dd binding was measured as HRP-dependent absorbance following incubation with the TMB substrate. Absorbance was measured at 450 nm. Each data point represents average and standard deviation from three independent measurements. Hyperbolic bindings curves were fitted and (C) apparent binding constants K_d^{app} extracted.

3.3 Imaging of Dd - lipid interaction

In our experiments performed hitherto, lipids were not presented in their recognition pattern as they are in the physiological context of biological membrane. Bearing this in mind, to verify Dd affinity to PS, CL and other anionic phospholipids we set up a line of experiments with liposomes. Liposomes have certain advantage over lipids immobilized or disposed on a support, because they are constituted by a continuous lipid bilayer, mimicking closer-to-natural lipid lateral organization.

Firstly, we prepared giant unilamellar vesicles (GUV), micrometer-sized liposomes, convenient for observation under optical microscope. To screen specific Dd-lipid interactions, we prepared GUVs composed of pure POPC and 60 mol% POPC doped with 40 mol% several negatively charged lipids or cholesterol (20 mol% in the case of PIP_3). Dd was detected by primary and secondary, fluorescently labeled antibodies or directly by Dd-A647 fluorescence. Fig. 4 shows that membrane-bound Dd could be detected only at the surface of POPS-doped vesicles. Similarly to previous experiments, reaction of lysine amine groups of Dd-A647 abolished Dd membrane binding.

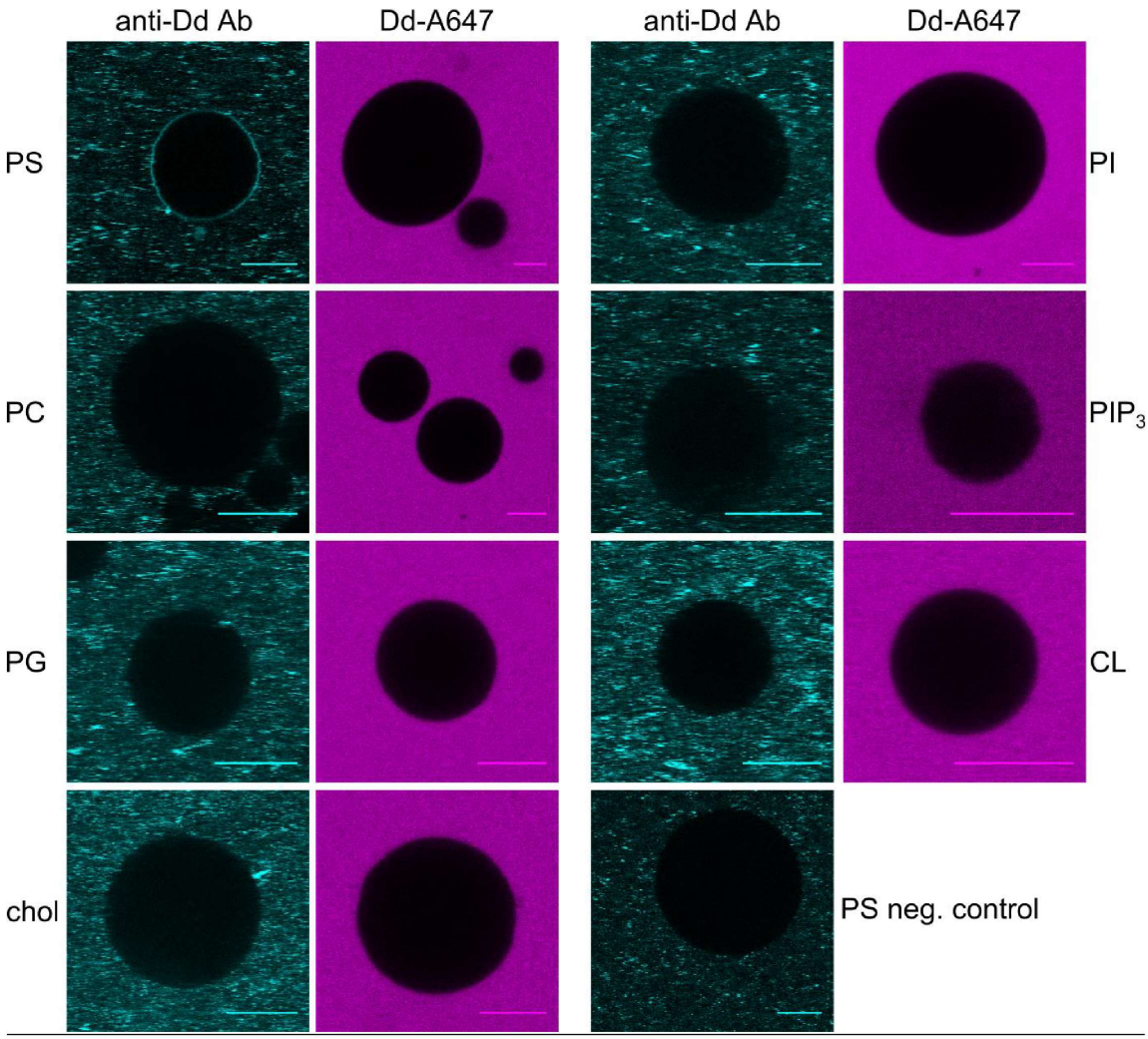

Fig. 4. Confocal microscopy analysis of giant unilamellar vesicles composed of pure PC and 40 mol% (PS, PG, chol, PI, CL) or 20 mol% addition (PIP_3) to PC incubated under identical conditions with unmodified Dd detected with antibodies: primary rabbit anti-Dd and secondary anti-rabbit Alexa Fluor-555 (anti-Dd Ab) (cyan) or direct fluorescence of Dd-Alexa647 conjugate (DdA647) (magenta). Negative control for PS (without Dd incubation) showed no unspecific lipid-antibody interactions. Scale bars 10 μm.

3.4. Dd affinity to negatively charged surfaces with carboxylic functional group

Secondly, we performed surface plasmon resonance (SPR) experiments with large unilamellar vesicles (LUVs) immobilized on the surface of L1 Biacore chip, containing carboxymethylated dextran with alkyl chains allowing for LUV disposal. This method requires the presence of a reference cell, used for the signal subtraction from the cell of interest. Ideally, it should be treated with the same

chemicals as other flow cells used in the study and do not exhibit analyte binding properties. When unmodified L1 surface was used as a reference, it was not possible to obtain the binding sensogram, because Dd showed the highest affinity to carboxymethylated dextran molecules containing negatively charged carboxyl groups (Suppl Fig. 1). However, assuming that the ~10-fold lower binding constants for PS observed in colorimetric assay are still valid for bilayers, it was possible to construct sensograms for carboxymethylated dextran and PC/PS 60/40 mol% LUVs using pure PC flow cell as a reference (Fig. 5). In fact, Dd did not show any symptoms of interactions with PC, because the sensograms were of a rectangular shape, characteristic for a passive flow over a surface (Suppl. Fig. 1C). In contrast, for both carboxymethylated dextran and PC/PS liposomes referenced with PC, the sensograms indicated Dd affinity to the surface, even higher for the carboxymethylated dextran (Fig. 5A and B, respectively), suggesting Dd affinity to negatively charged carboxylic groups present in PS as well as in dextran.

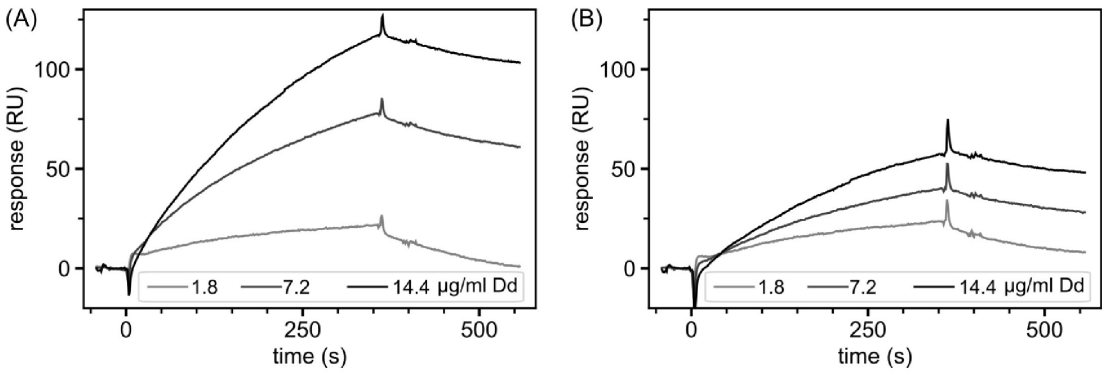

Fig. 5. Surface plasmon resonance analysis. Ad3 Dd binding to negatively charged surfaces of (A) carboxymethylated dextran L1 chip surface, (B) PC/PS 60/40 mol% LUVs disposed onto chip surface. In both cases a surface covered by POPC vesicles was used as a reference.

3.5. PS blocking in PS exposing viable cancer cells affects Dd endocytosis

With the aim of blocking PS exposed on cell surface, we evaluated internalization of Dd following the preincubation of human astrocytoma cells (U-251 MG, formally known U-373 MG) with Annexin V-FITC (AnnV-FITC). The Ann V-FITC binding to non-apoptotic cells U-251 MG, exhibiting elevated PS levels, was revealed by flow cytometry analysis [16]. However, plasma-membrane bound AnnV-FITC was not observed by means of fluorescence microscopy imaging and was at the level of cellular autofluorescence (Suppl. Fig. 2). Most likely, under these conditions the amount of membrane bound

AnnV-FITC is below the detection threshold. Yet this opens the opportunity of cellular localization of Dd detection with specific primary and secondary antibody labeled with Alexa Fluor 488, emitting in the same spectral channel as AnnV-FITC. Under the same imaging conditions, the signal from internalized Dd is prevalent (Suppl. Fig. 2).

The cellular localization of Dd was monitored and quantified by confocal microscopy similarly as in previous experiments (Fig. 1). Confocal images of U-251 MG cells incubated at 4 °C (Fig. 6A), namely under conditions of inhibited receptor-mediated endocytosis, demonstrated green fluorescent signal from Dd overlapping with plasma membrane. Fluorescence intensity was comparable for cells preincubated with AnnV and cells incubated solely with Dd (Fig. 6A). We did not observe significant differences between those two specimens (Fig. 6A, right panel). However, the results obtained for cells incubated at 37 °C (Fig. 6B) demonstrated significant, about 70% fluorescence signal reduction in cells treated with PS-binding reagent (Fig 6B, right panel). This result clearly shows that blocking of PS at the cell surface has an impact on the endocytotic uptake of Dd.

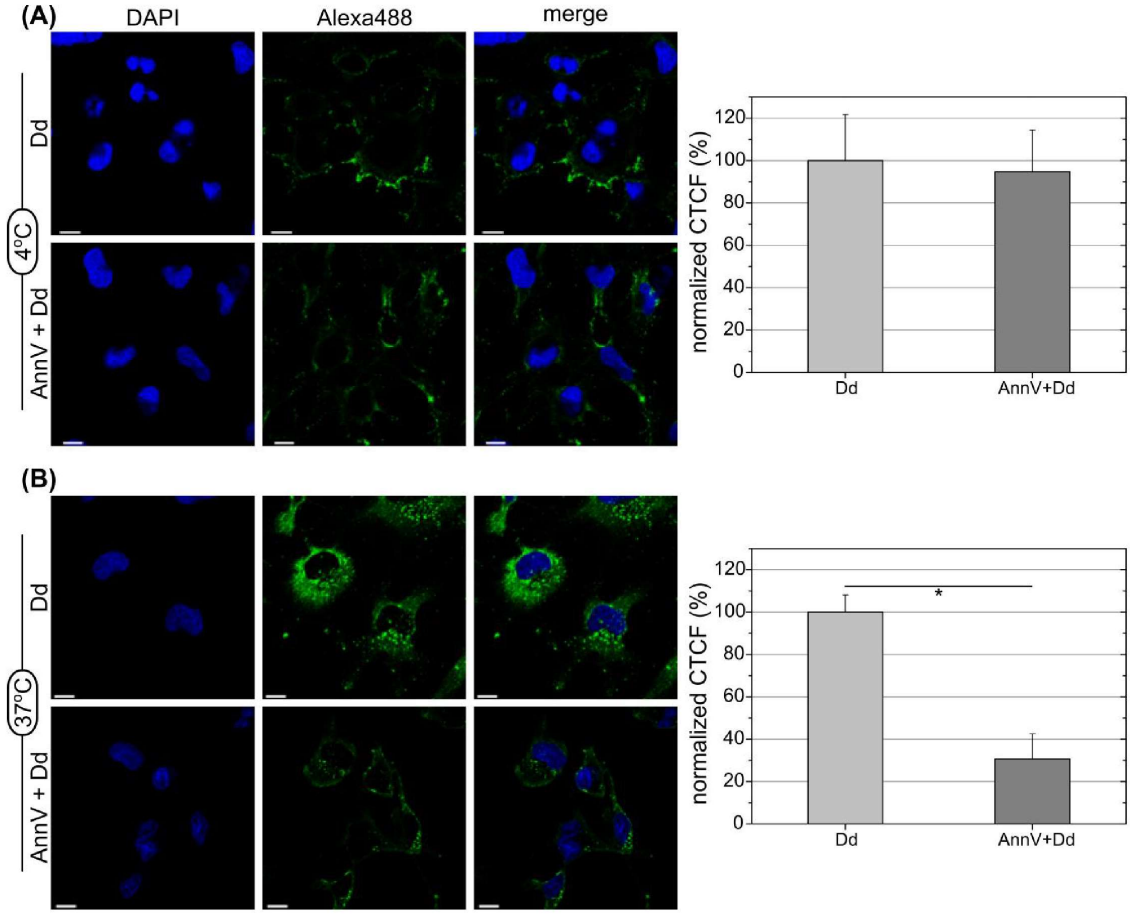

Fig. 6. Confocal microscopy analysis of U 251 MG cells preincubated with Annexin V for 15 min prior to incubation with Dd (AnnV+Dd) or incubated solely with Dd for 2 h at 4°C (A, left panel) or at

37°C (B, left panel). Cell nuclei were stained blue with DAPI (5 μg/ml), Dd was detected with the primary anti-Dd antibody and Alexa Fluor 488 conjugated secondary antibody (Alexa 488, green). Scale bar is 10 μm. The confocal microscope settings were kept the same between samples. Contrast and brightness of all samples and controls were adjusted simultaneously. Right panels: the quantitative analysis of confocal microscopy results representing mean values expressed as a percentage of CTCF for cells incubated with Dd in comparison to cells treated with AnnV+Dd for 2 h at 4°C (A, right panel) or at 37°C (B, right panel). Data represents mean values and error bars refer to standard deviations (*- p-value < 0.001, two-sided T-test).

4. Discussion

Lipids that are the main component of cellular membranes, are highly diverse in structure, and their distribution varies at the level of organism, cell type, organelle, and bilayer leaflet. The majority of phospholipids present in cell membranes constitute neutral phosphoglycerides such as phosphatidylcholine (PC) and phosphatidylethanolamine (PE), however negatively charged phospholipids such as phosphatidylserine (PS), phosphatidylinositol (PI), phosphatidic acid (PA) and phosphatidylglycerol (PG) are the essential structural components involved in specific interactions with proteins containing positively charged amino acid side chains.

Here, we focused on the interactions between membrane lipids and self-assembling particle, Dd, composed solely of twelve copies of penton base protein, derived from HAd3 capsid, which is responsible for the virus internalization to host cells and is considered as a potential drug delivery vector [3–5,9,10,17]. Adenoviruses cell penetration by clathrin-dependent endocytosis [18] may be mediated by low-density lipoprotein receptors, negatively charged phospholipids and gangliosides that all have been shown to assist entry of different viruses [19] (and references therein: [20–24]). Wide range of cells penetrated efficiently by Dd, prompted us to suspect that there may be membrane components other than known Dd receptors or other endocytic clathrin-independent pathways, that are engaged in cell penetration, depending on the cell type.

Cholesterol, the most abundant lipid component of the plasma membrane, plays a key role in organizing lipid rafts that serve as a platform for viruses to enter cells [19] and is essential in clathrin-dependent Ad2 endocytosis [25]. It has been observed that Ads infection in the presence of free cholesterol led to increased binding, uptake, and expression of viruses [26]. Methyl-β-cyclodextrin has been widely used to deplete plasma membrane cholesterol from cells, leading to inhibition of endocytic pathways including macropinocytosis, caveolin-dependent and clathrin-mediated endocytosis. Here, we presented that, cholesterol reduction with methyl-β-cyclodextrin strongly impaired Dd cell entry (Fig. 1), similarly to Ad2 and Ad5, for which it has been shown that the depletion of cholesterol in HeLa cells inhibited rapid endocytosis, endosomal escape, and nuclear targeting [25]. Notwithstanding, we did not observe direct interaction between Dd particles and

cholesterol neither during protein-lipid overlay nor analyzing Dd-GUV interaction, which is consistent with the prediction that cholesterol is indirectly involved in Dd cell penetration. The low rate internalization of Dd observed after cholesterol depletion may also suggest an alternative clatrin-independent low-capacity entry pathway, however it requires further confirmation and deeper studies.

Model membranes such as unilamellar vesicles are highly suitable for evaluation of the affinity of indicated protein to lipid bilayer and allowed us to study biophysical interactions using various techniques, such as microscopy imaging or surface plasmon resonance (SPR). Liposomes may be considered as a model cell membranes in which the lipid organization mimics the arrangement of lipids in natural cell membranes, e.g. the zwitterionic lipid system consisting of PC may act as a mimic of the outer leaflet of healthy eukaryotic cells while the anionic system (PC/PS) may corresponds to the enhanced anionic character of cancer or apoptotic cells that expose PS. Interactions of adenoviral penton base protein and PS has not been described hitherto. We speculate that PS may play enhancing role in entry to cancer cells externally exposing PS. Viable cancer and tumor-associated vascular cells expose on their surface elevated levels of negatively charged PS upon malignant transformation [27,28]. It was found that differential flippase activity and intracellular calcium concentration are the major regulators of this phenomenon in viable human cancer cells [29]. Cancer cell lines that highly expose PS on their surface exhibit weak flippase activity and high intracellular calcium, whereas cancer cells with low surface PS exhibited high flippase activity and low intracellular calcium. Cancer cells that externally expose PS display also a higher total cellular PS level [29]. Thus, Dd – PS interaction is a feature to be considered in the design of Dd-based delivery tools and may have an impact on elucidation of lipid-mediated cell entry.

Interestingly, while modifying Dd by NHS-based conjugation of the primary amine of lysine residues NHS-ester of Alexa Fluor fluorescent dye, we observed that interaction with PS was strongly affected as compared to unmodified particle (Fig. 2). This may indicate that positively charged amino acids such as lysines or arginines are directly involved in the interaction with this anionic phospholipid. Dd, which is a homooligomer contains two external loops in the structure of each Pb monomer, namely the variable loop and the RGD loop. One K and two R residues are present in the variable loop, while the RGD loop contains three K and two R residues [30]. Moreover, in the structure of Dd we can distinguish a basic motif RKR present in the waist-like groove of Pb penton (Fig. 7). Theoretically, NHS-ester of Alexa647 could attach to each lysine exposed on Dd surface, however the comparison of tryptic peptide patterns of unmodified Dd and Dd-Alexa647 conjugate suggests that fluorescent dye is conjugated only to K339 located in RGD-loop and K272 located in positively charged RKR motif (data not shown). Modification of lysine residues that are adjacent to arginine residues in both predicted regions results in a steric hindrance and may also affect direct interaction with arginine, therefore it is impossible to rule out the role of this positively charged amino acid in lipid binding without having Dd mutants

lacking K or R in predicted sites. Pointing individual residues involved in the interaction with Dd requires further research and mutagenesis. The conclusions drawn from SPR experiments lead us to the prediction that it may be a negatively charged carboxyl group present both in dextran as well as PS structure that is responsible for specific interaction with basic amino acids. It is worth noticing that the carboxyl head group differentiates PS from other negatively charged phospholipids for which we did not observe specific interaction with Dd.

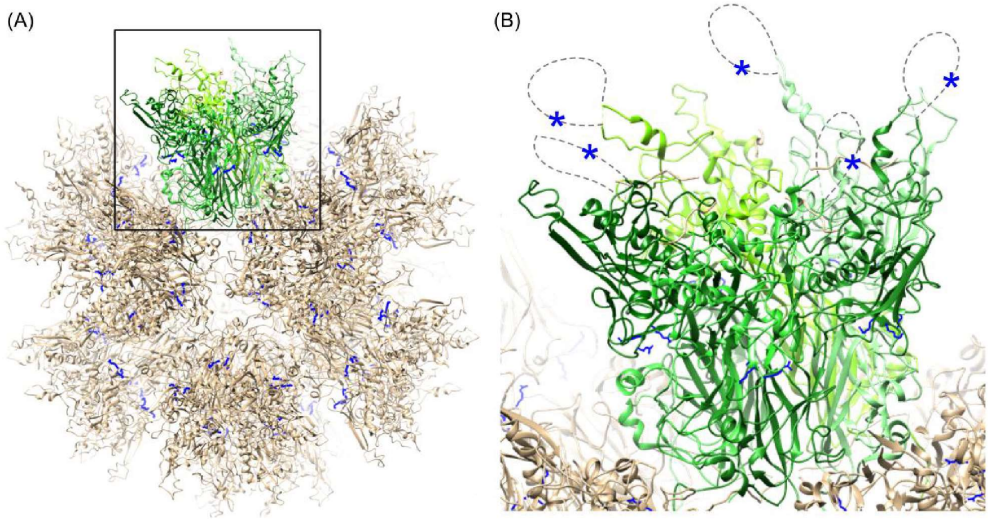

Fig. 7. (A) Structure of Human adenoviral dodecahedron (PDB ID: 4AQQ) and (B) zoom of a single pentameric penton base protein (green) with basic RKR motifs (marked blue) and RGD loop (dashed gray), missing in crystal structure, containing basic KQKR sequence (blue star). Structures rendered in Chimera software [31].

Since we proved by various methods that Dd-PS interaction is the only direct and specific among other ones, our next goal was to evaluate the role of PS on cellular level. As a proof of concept, we performed experiments using human astrocytoma U-251 MG, since it is the cell line known for the exposure of elevated levels of PS in the outer leaflet of cell membrane [16]. We think that the observed relationship between PS-blocking and internalization efficiency may be the rationale standing behind cell-type specific Dd penetration.

Ackowledgements

We are grateful to Malgorzata Lichocka (Institute of Biochemistry and Biophysics, Polish Academy of Sciences, Warsaw) for help in confocal microscopy imaging (Fig. 1 and 6) and Anton Slyvka (International Institute of Molecular and Cell Biology, Warsaw) for rendering of Dd structures (Fig. 7). We acknowledge the help of Krzysztof Skowronek (International Institute of Molecular and Cell Biology, Warsaw) in accessing Biacore 3000 (GE Healthcare).

Funding

This work was funded by the National Science Centre grants:[UMO-2012/07/D/NZ1/04255] to RW, and [DEC-2013/09/B/NZ3/02327] to ES and by grant from Association Espoire to JC. This work was partially performed in the NanoFun laboratories co-financed by the European Regional Development Fund within the Innovation Economy Operational Program, project no. POIG.02.02.00-00- 025/09/.

Conflict of interest statement

None declared

References

1. Szurgot, I.; Szolajska, E.; Laurin, D.; Lambrecht, B.; Chaperot, L.; Schoehn, G.; Chroboczek, J. Self-adjuvanting influenza candidate vaccine presenting epitopes for cell-mediated immunity on a proteinaceous multivalent nanoplatform. *Vaccine* **2013**, *31*, 4338–4346, doi:10.1016/j.vaccine.2013.07.021.

2. Naskalska, A.; Szolajska, E.; Chaperot, L.; Angel, J.; Plumas, J.; Chroboczek, J. Influenza recombinant vaccine: Matrix protein M1 on the platform of the adenovirus dodecahedron. *Vaccine* **2009**, *27*, 7385–7393, doi:10.1016/j.vaccine.2009.09.021.

3. Zochowska, M.; Piguet, A. C.; Jemielity, J.; Kowalska, J.; Szolajska, E.; Dufour, J. F.; Chroboczek, J. Virus-like particle-mediated intracellular delivery of mRNA cap analog with in vivo activity against hepatocellular carcinoma. *Nanomedicine Nanotechnology, Biol. Med.* **2015**, *11*, 67–76, doi:10.1016/j.nano.2014.07.009.

4. Zochowska, M.; Paca, A.; Schoehn, G.; Andrieu, J. P.; Chroboczek, J.; Dublet, B.; Szolajska, E. Adenovirus dodecahedron, as a drug delivery vector. *PLoS One* **2009**, *4*, doi:10.1371/journal.pone.0005569.

5. Fender, P.; Ruigrok, R. W. H.; Gout, E.; Buffet, S.; Chroboczek, J. Adenovirus dodecahedron, a new vector for human gene transfer. *Nat. Biotechnol.* **1997**, *15*, 52–56, doi:10.1038/nbt0197-52.

6. Vivès, R. R.; Lortat-Jacob, H.; Chroboczek, J.; Fender, P. Heparan sulfate proteoglycan mediates the selective attachment and internalization of serotype 3 human adenovirus dodecahedron. *Virology* **2004**, *321*, 332–340, doi:10.1016/j.virol.2004.01.015.

7. Fender, P.; Schoehn, G.; Perron-Sierra, F.; Tucker, G. C.; Lortat-Jacob, H. Adenovirus dodecahedron cell attachment and entry are mediated by heparan sulfate and integrins and vary along the cell cycle. *Virology* **2008**, *371*, 155–164, doi:10.1016/j.virol.2007.09.026.

8. Gout, E.; Schoehn, G.; Fenel, D.; Lortat-Jacob, H.; Fender, P. The adenovirus type 3 dodecahedron's RGD loop comprises an HSPG binding site that influences integrin binding. *J. Biomed. Biotechnol.* **2010**, *2010*, 541939, doi:10.1155/2010/541939.

9. Garcel, A.; Gout, E.; Timmins, J.; Chroboczek, J.; Fender, P. Protein transduction into human cells by adenovirus dodecahedron using WW domains universal adaptors. *J. Gene Med.* **2006**, *8*, 524–531, doi:10.1002/jgm.862.

10. Jedynak, M.; Laurin, D.; Dolega, P.; Podsiadla-Bialoskorska, M.; Szurgot, I.; Chroboczek, J.; Szolajska, E. Leukocytes and drug-resistant cancer cells are targets for intracellular delivery by adenoviral dodecahedron. *Nanomedicine* **2018**, *14*, 1853–1865, doi:10.1016/j.nano.2018.05.001.

11. Ran, S.; Downes, A.; Thorpe, P. E. Increased Exposure of Phosphatidylethanolamine on the Surface of Tumor Vascular Endothelium. *Cancer Res.* **2002**, *62*, 3132–3140, doi:10.1593/neo.101366.

12. Szurgot, I.; Jedynak, M.; Podsiadla-Bialoskorska, M.; Piwowarski, J.; Szolajska, E.; Chroboczek, J. Adenovirus Dodecahedron, a VLP, Can be Purified by Size Exclusion Chromatography Instead of Time-Consuming Sucrose Density Gradient Centrifugation. *Mol. Biotechnol.* **2015**, *57*, 565–573, doi:10.1007/s12033-015-9850-9.

13. Angelova, M. I.; Dimitrov, D. S. Liposome electroformation. *Faraday Discuss. Chem. Soc.* **1986**, *81*, 303–311, doi:10.1039/DC9868100303.

14. Czogalla, A.; Grzybek, M.; Jones, W.; Coskun, U. Validity and applicability of membrane model systems for studying interactions of peripheral membrane proteins with lipids. *Biochim. Biophys. Acta* **2013**, doi:10.1016/j.bbalip.2013.12.012.

15. Kooijman, E. E.; King, K. E.; Gangoda, M.; Gericke, A. Ionization properties of phosphatidylinositol polyphosphates in mixed model membranes. *Biochemistry* **2009**, *48*, 9360–9371, doi:10.1021/bi9008616.

16. Vallabhapurapu, S. D.; Blanco, V. M.; Sulaiman, M. K. Variation in human cancer cell external phosphatidylserine is regulated by flippase activity and intracellular calcium. *Oncotarget* **2015**, *6*, doi:10.18632/oncotarget.6045.

17. Sumarheni; Gallet, B.; Fender, P. The Use of Adenovirus Dodecahedron in the Delivery of an Enzymatic Activity in the Cell. *Biotechnol. Res. Int.* **2016**, *2016*, 5030589, doi:10.1155/2016/5030589.

18. Meier, O.; Boucke, K.; Hammer, S. V.; Keller, S.; Stidwill, R. P.; Hemmi, S.; Greber, U. F. Adenovirus triggers macropinocytosis and endosomal leakage together with its clathrin-mediated uptake. *J. Cell Biol.* **2002**, *158*, 1119–1131, doi:10.1083/jcb.200112067.

19. Mazzon, M.; Mercer, J. Lipid interactions during virus entry and infection. *Cell. Microbiol.* **2014**, *16*, 1493–1502, doi:10.1111/cmi.12340.

20. Tsai, B.; Gilbert, J. M.; Stehle, T.; Lencer, W.; Benjamin, T. L.; Rapoport, T. A. Gangliosides are receptors for murine polyoma virus and SV40. *EMBO J.* **2003**, *22*, 4346–4355, doi:10.1093/emboj/cdg439.

21. Campanero-Rhodes, M. A.; Smith, A.; Chai, W.; Sonnino, S.; Mauri, L.; Childs, R. A.; Zhang, Y.; Ewers, H.; Helenius, A.; Imberty, A.; Feizi, T. N-Glycolyl GM1 Ganglioside as a Receptor for Simian Virus 40. *J. Virol.* **2007**, *81*, 12846–12858, doi:10.1128/JVI.01311-07.

22. Roth, S. L.; Whittaker, G. R. Promotion of vesicular stomatitis virus fusion by the endosome-specific phospholipid bis(monoacylglycero)phosphate (BMP). *FEBS Lett.* **2011**, *585*, 865–869, doi:10.1016/j.febslet.2011.02.015.

23. Izquierdo-Useros, N.; Lorizate, M.; Contreras, F. X.; Rodriguez-Plata, M. T.; Glass, B.; Erkizia, I.; Prado, J. G.; Casas, J.; Fabriàs, G.; Kräusslich, H. G.; Martinez-Picado, J. Sialyllactose in viral membrane gangliosides is a novel molecular recognition pattern for mature dendritic cell capture of HIV-1. *PLoS Biol.* **2012**, *10*, doi:10.1371/journal.pbio.1001315.

24. Meisen, I.; Dzudzek, T.; Ehrhardt, C.; Ludwig, S.; Mormann, M.; Rosenbrück, R.; Lümen, R.; Kniep, B.; Karch, H.; Müthing, J. The human H3N2 influenza viruses A/Victoria/3/75 and A/Hiroshima/52/2005 preferentially bind to α2-3-sialylated monosialogangliosides with fucosylated poly-N-acetyllactosaminyl chains. *Glycobiology* **2012**, *22*, 1055–1076, doi:10.1093/glycob/cws077.

25. Imelli, N.; Meier, O.; Boucke, K.; Hemmi, S.; Greber, U. F. Cholesterol Is Required for Endocytosis and Endosomal Escape of Adenovirus Type 2. *J. Virol.* **2004**, *78*, 3089–3098, doi:10.1128/JVI.78.6.3089-3098.2004.

26. Worgall, S.; Worgall, T. S.; Kostarelos, K.; Singh, R.; Leopold, P. L.; Hackett, N. R.; Crystal,

R. G. Free Cholesterol Enhances Adenoviral Vector Gene Transfer and Expression in CAR-Deficient Cells. *Mol. Ther.* **2000**, *1*, 39–48, doi:10.1006/mthe.1999.0013.

27. Ran, S.; Thorpe, P. E. Phosphatidylserine is a marker of tumor vasculature and a potential target for cancer imaging and therapy. *Int. J. Radiat. Oncol.* **2002**, *54*, 1479–1484, doi:10.1016/S0360-3016(02)03928-7.

28. Zwaal, R. F. A.; Comfurius, P.; Bevers, E. M. Surface exposure of phosphatidylserine in pathological cells. *Cell. Mol. Life Sci.* **2005**, *62*, 971–988, doi:10.1007/s00018-005-4527-3.

29. Coil, D. A.; Miller, A. D. Phosphatidylserine Is Not the Cell Surface Receptor for Vesicular Stomatitis Virus ~~Phosphatidylserine Is Not the Cell Surface Receptor for Vesicular Stomatitis Virus~~. *J. Virol.* **2004**, *78*, 10920–10926, doi:10.1128/JVI.78.20.10920.

30. Szolajska, E.; Burmeister, W. P.; Zochowska, M.; Nerlo, B.; Andreev, I.; Schoehn, G.; Andrieu, J. P.; Fender, P.; Naskalska, A.; Zubieta, C.; Cusack, S.; Chroboczek, J. The Structural Basis for the Integrity of Adenovirus Ad3 Dodecahedron. *PLoS One* **2012**, *7*, 1–11, doi:10.1371/journal.pone.0046075.

31. Pettersen, E. F.; Goddard, T. D.; Huang, C. C.; Couch, G. S.; Greenblatt, D. M.; Meng, E. C.; Ferrin, T. E. UCSF Chimera - A visualization system for exploratory research and analysis. *J. Comput. Chem.* **2004**, *25*, 1605–1612, doi:10.1002/jcc.20084.

Supplementary Material

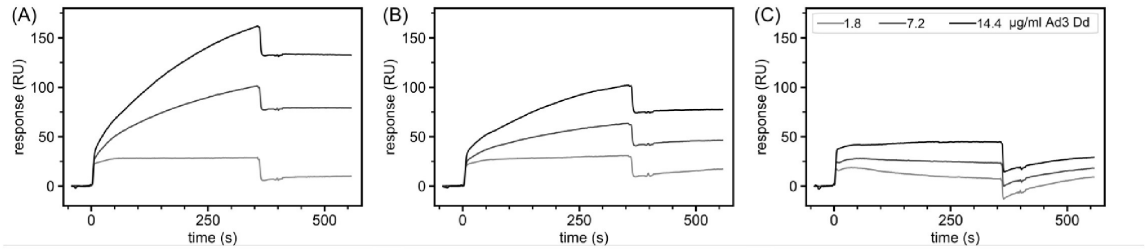

Suppl Fig. 1. Absolute resonance signals registered during Ad3 Dd flow over (A) unmodified carboxymethylated dextran surface of L1 chip, (B) PC/PS 60/40 mol% LUVs, (C) PC LUVs.

Imaging of U-251 cells

Control samples were prepared as follows: U-251, non-treated cells. U-251 + I+IIAF488, cells incubated with the polyclonal rabbit anti-Dd serum diluted 1:1,000 1 h at RT and the Alexa Fluor 488-

conjugated chicken anti-rabbit IgG diluted 1:500 for 1 h at RT. U-251 + IIAF488, cells incubated with secondary antibody Alexa Fluor 488- conjugated chicken anti-rabbit IgG diluted 1:500 for 1 h at RT. U-251 + AnnV, , cells incubated in dark for 15 min with 5 µl of Annexin V-FITC (AnnV) (20 µg/ml) diluted in 200 µl of annexin binding buffer. U-251 + AnnV + Dd, cells incubated in dark for 15 min with 5 µl of Annexin V-FITC (AnnV) (20 µg/ml) diluted in 200 µl of Annexin binding buffer, prior to incubation with 10 µg Dd diluted in annexin binding buffer (20 µg /mL) for 2 h at 37 °C, Dd was detected with polyclonal rabbit anti-Dd serum and the Alexa Fluor 488- conjugated chicken anti-rabbit IgG. U-251 + Dd, cells incubated with 10 µg Dd diluted in annexin binding buffer (20 µg /mL) for 2 h at 37 °C, Dd was detected with polyclonal rabbit anti-Dd serum and the Alexa Fluor 488- conjugated chicken anti-rabbit IgG. The images were captured using Nikon Eclipse E800 epifluorescence microscope. DAPI and Alexa Fluor 488 fluorescence was excited at 340-380 nm and 465-495 nm, and emission was measured at 435- 485 and 515-555 nm, respectively. Images shown in Suppl Fig. 2. were processed with ImageJ software and were selected as representatives and adjusted simultaneously.

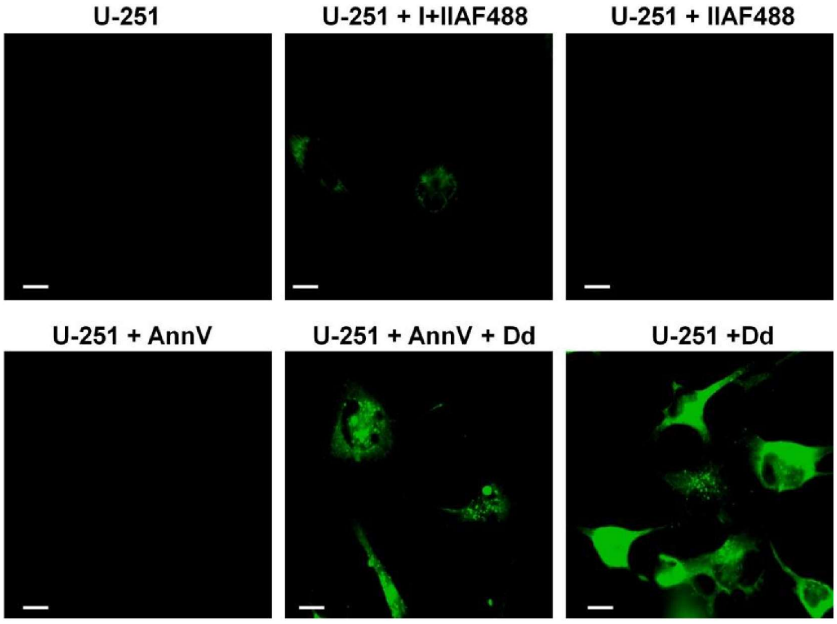

Suppl Fig. S2. Fluorescence microscopy analysis of controls: U-251, non-treated cells. U-251 + I+IIAF488, cells incubated with the polyclonal rabbit anti-Dd serum diluted 1:1,000 1 h at RT and the Alexa Fluor 488- conjugated chicken anti-rabbit IgG diluted 1:500 for 1 h at RT. U-251 + IIAF488, cells incubated with secondary antibody Alexa Fluor 488- conjugated chicken anti-rabbit IgG diluted 1:500 for 1 h at RT. U-251 + AnnV, cells incubated in dark for 15 min with 5 µl of Annexin V-FITC (AnnV) (20 µg/ml) diluted in 200 µl of annexin binding buffer. U-251 + AnnV + Dd, cells incubated in dark for 15 min with 5 µl of Annexin V-FITC (AnnV) (20 µg/ml) diluted in 200 µl of annexin

binding buffer, prior to incubation with 10 µg Dd diluted in annexin binding buffer (20 µg /ml) for 2 h at 37 °C, Dd was detected with polyclonal rabbit anti-Dd serum and the Alexa Fluor 488- conjugated chicken anti-rabbit IgG. U-251 + Dd, cells incubated with 10 µg Dd diluted in annexin binding buffer (20 µg /ml) for 2 h at 37 °C, Dd was detected with polyclonal rabbit anti-Dd serum and the Alexa Fluor 488- conjugated chicken anti-rabbit IgG. Scale bar 10 µm.